ARMY RESEARCH LABORATORY

Distributed Detection of Binary Decisions with Collisions in a Large, Random Network

by Gene T. Whipps, Emre Ertin, and Randolph L. Moses

ARL-TR-6678 September 2013

NOTICES

Disclaimers

The findings in this report are not to be construed as an official Department of the Army position unless so designated by other authorized documents.

Citation of manufacturer's or trade names does not constitute an official endorsement or approval of the use thereof.

Destroy this report when it is no longer needed. Do not return it to the originator.

Army Research Laboratory

Adelphi Laboratory Center, MD 20783-1138

ARL-TR-6678 **September 2013**

Distributed Detection of Binary Decisions with Collisions in a Large, Random Network

Gene T. Whipps

Sensors & Electron Devices Directorate, ARL

Emre Ertin and Randolph L. Moses

Department of Electrical & Computer Engineering, The Ohio State University

REPORT DOCUMENTATION PAGE	Form Approved OMB No. 0704-0188

1. REPORT DATE *(DD-MM-YYYY)*	2. REPORT TYPE	3. DATES COVERED (From - To)
September 2013	Final	

4. TITLE AND SUBTITLE	5a. CONTRACT NUMBER
Distributed Detection of Binary Decisions with Collisions in a Large, Random Network	5b. GRANT NUMBER
	5c. PROGRAM ELEMENT NUMBER

6. AUTHOR(S)	5d. PROJECT NUMBER
Gene T. Whipps Emre Ertin Randolph L. Moses	5e. TASK NUMBER
	5f. WORK UNIT NUMBER

7. PERFORMING ORGANIZATION NAME(S) AND ADDRESS(ES)	8. PERFORMING ORGANIZATION REPORT NUMBER
U.S. Army Research Laboratory ATTN: RDRL-SES-A Adelphi, MD 20783-1138	ARL-TR-6678

9. SPONSORING/MONITORING AGENCY NAME(S) AND ADDRESS(ES)	10. SPONSOR/MONITOR'S ACRONYM(S)
	11. SPONSOR/MONITOR'S REPORT NUMBER(S)

12. DISTRIBUTION/AVAILABILITY STATEMENT

Approved for public release; distribution is unlimited.

13. SUPPLEMENTARY NOTES

primary author's email: <gene.t.whipps.civ@mail.mil>

14. ABSTRACT

We consider the problem of distributed detection in a large network of sensors under network communication constraints. Sensor nodes are randomly deployed and follow a random sleep/wake schedule. When awake, sensor nodes perform local detection tests and communicate detections over a multiple-access channel to a fusion center. The fusion center can detect both successful communications and communication collisions in the channel. We derive fusion rules for perfect communications and a delay-constrained protocol and show that each are functions of count statistics only. We derive analytical expressions that characterize the performance of the system in terms of energy consumption and detection probability. Simulation examples compare theoretical predictions with numerical results.

15. SUBJECT TERMS

Distributed detection, binary sensors, random access sensor network

16. SECURITY CLASSIFICATION OF:			17. LIMITATION OF ABSTRACT	18. NUMBER OF PAGES	19a. NAME OF RESPONSIBLE PERSON
a. REPORT	b. ABSTRACT	c. THIS PAGE			Gene T. Whipps
Unclassified	Unclassified	Unclassified	UU	37	19b. TELEPHONE NUMBER (*Include area code*) 301-996-5604

Contents

List of Figures

List of Tables

1. Introduction

This report considers the problem of distributed detection in a large, random network of sensor nodes. We consider a localized event and focus on the case where sensor nodes communicate binary decisions over a single-hop wireless network to a common fusion node. The fusion node combines the received information in order to make a global decision on the presence or absence of a signal source.

This work is related to and draws from recent works in distributed detection. Niu et al. [1] show that, if local decisions are communicated perfectly, the fusion rule for independent and identically distributed (i.i.d.) binary observations, conditioned on the true hypothesis, simplifies to counting the number of detections. In reference 2, Niu et al. provide analytic and approximate expressions for the counting rule in a large, random sensor network and a random target location. Chang et al. [3] incorporate a random access protocol for a fixed number of sensor nodes, and they derive a fusion rule that is a weighted sum of the number of 1's and 0's successfully received at the fusion node. Similarly, Kapnadak et al. [4] incorporate a random access protocol, but for a random sensor network. Aldalahmeh et al. [5] develop a real-time counting rule and provide an approximation to the system performance assuming that collisions are negligible. Similar to references 2, 4, and 5, we consider a large, random sensor network and incorporate a random access protocol. In contrast, however, we assume a sensor node transmits only when it declares a detection (i.e., when a node decides a signal source is present). As a result, collisions from simultaneous communications imply that at least two sensor nodes are attempting to transmit detection messages. While other works attempt to fuse local decisions through counts of 1's and 0's that are successfully received, this work derives the fusion rule for successfully transmitted 1's and a count statistic on collisions. For comparison, we re-derive the fusion rule assuming the local decisions are communicated perfectly [2].

The remainder of this report is outlined as follows. In section 2, we outline the sensor network model, including the local sensor operation, and the network communication model. Then in section 3, we derive the fusion rules for the case of perfect communications and a given delay-constrained communications protocol. In section 4, we discuss the system performance as a function of the density of the sensor network. We derive a bound on the vertical uncertainty of the receiver operating characteristics in section 5. We present numerical examples in section 6 validating the analytic results and comparing with previous results under perfect communications. Finally, conclusions are given in section 7.

2. Network System Model

In this section, we describe the sensor network model, including the local sensor operation, the network communication model, and the fusion node processing. We assume a large number of sensor nodes are randomly deployed independently and uniformly over a bounded, circular region. Each node awakens with some probability at each time interval, and if active, senses its environment, computes a local decision, and communicates any detections to the fusion node using a delay-constrained media access control (MAC) protocol. When multiple nodes attempt to communicate over a shared wireless communications medium, transmitted messages are subject to errors due to collisions with other ongoing message transmissions. Therefore, the fusion node must take this into account when forming a decision rule.

As a matter of notation, unless otherwise specifically stated, random variables are denoted with uppercase letters, specific outcomes are represented by lowercase letters, and bold letters represent vectors. For example, X is a random variable while $\underline{X} = [X_1, \ldots, X_n]^{\mathrm{T}}$ is a random vector with exactly n elements.

2.1 Sensor Network Model

Sensor nodes are deployed randomly, independently and uniformly over circular region $\mathcal{R}$. Without loss of generality, we assume $\mathcal{R} \in \mathbb{R}^2$ is centered at $(0, 0)$ with given radius $r < \infty$. Figure 1 depicts a random sensor network deployment with a fusion node centered in region $\mathcal{R}$. The locations of the signal source and sensor i are denoted by $\underline{L}_s$ and $\underline{L}_i$, respectively, with Euclidean distance between them given by $D_i = \|\underline{L}_i - \underline{L}_s\|$. The sensor locations $\{\underline{L}_i\}$ are i.i.d. with known distribution – uniform on $\mathcal{R}$. It follows that for any given location of the signal source, the distances $\{D_i\}$ between the signal source and the sensors are conditionally i.i.d.

To conserve energy, each sensor node follows a random sleep/wake schedule, independent of all other nodes. Let $\mathbb{N}_0 = \{0, 1, 2, \ldots\}$, the set of non-negative integers. The number of active nodes N during any activity period is modeled according to

$$\Pr(N = n) = e^{-\lambda} \frac{\lambda^n}{n!}, \quad n \in \mathbb{N}_0, \tag{1}$$

where $\lambda \in (0, \infty)$ is the average number of active nodes in region $\mathcal{R}$. We assume activity periods are non-overlapping and have a fixed and known duration. From the above properties, active sensor nodes represent a homogeneous Poisson point process (PPP).

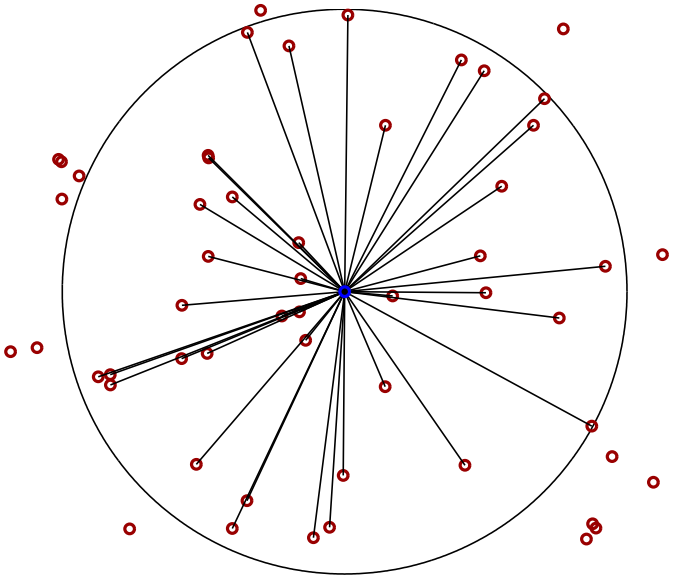

Figure 1. A random sensor network deployment with links to a fusion node centered in region $\mathcal{R}$ with radius r.

Each active sensor node senses its environment and makes a local detection decision. Sensors collect noisy measurements of the environment for the purpose of detecting whether or not a source signal is present in the scene. Under the null hypothesis h_0, when no signal is present, sensors measure only noise. We assume the observations are i.i.d. given h_0 is the true state of nature. The conditional joint distribution of the sensor observations under h_0 is given by

$$f_{\underline{X}|N,H}\left(\underline{x}|n,h_0\right) = \prod_{i=1}^{n} f_{X|H}\left(x_i|h_0\right), \tag{2}$$

where $\underline{X} = [X_1, \ldots, X_n]^{\mathrm{T}}$, $\underline{x} = [x_1, \ldots, x_n]^{\mathrm{T}}$ with $x_i \in \mathbb{R}$ for $i = 1, 2, \ldots, n$, and $\underline{x}$ is a realization of $\underline{X}$. We do not consider the more general case, where $x_i \in \mathbb{R}^m$ with $m \geq 1$. Here, x_i could, for example, represent the output of an energy detector at node i.

Under the alternative hypothesis h_1, in which a source is present, each sensor measures a source signal embedded in noise. We model the observations under h_1 to be conditionally i.i.d. according to

$$f_{\underline{X}|\underline{A},N,H}\left(\underline{x}|\underline{a},n,h_1\right) = \prod_{i=1}^{n} f_{X|\underline{A},H}\left(x_i|\underline{a},h_1\right), \tag{3}$$

given n active nodes and the signal vector $\underline{a} = [a_1, \ldots, a_n]^{\mathrm{T}}$, where $\underline{a}$ is a realization of the

random signal vector $\underline{A} = [A_1, \ldots, A_n]^{\mathrm{T}}$. Each A_i is an attenuated version of the scalar signal level $A_s > 0$ originating from the source. We assume a homogeneous medium that attenuates the source's signal in a manner that does not depend on the orientation relative to the source. We model the signal at sensor i as $A_i := A_s g(D_i) > 0$, where $g : [0, \infty) \to (0, \infty)$ models the attenuation as the signal propagates from the source and is a non-increasing function of distance. The attenuation factor g can model, for example, spherical spreading.

We assume the source's level A_s and location $\underline{L}_s$ are random with known distributions and are mutually independent along with N, $\{\underline{L}_i\}$, and sources of noise in sensor observations. Since $\{\underline{L}_i\}$ are i.i.d., it follows that the random variables A_i are identically distributed, while $\{A_i\}$ are not necessarily mutually independent. Let (R_s, Θ_s) represent the polar coordinates of the signal source located at $\underline{L}_s$. It was shown in reference 6 that $\{A_i\}$ are conditionally independent of the angle Θ_s and therefore i.i.d. given R_s, A_s, and N. We define a set $\mathcal{P} = (0, \infty) \times [0, r]$ and signal parameter vector $\underline{\Phi} = [A_s, R_s]^{\mathrm{T}} \in \mathcal{P}$ with probability distribution $f_{\underline{\Phi}}$. The conditional joint distribution of the signal at the sensors is then given by

$$f_{\underline{A}|\underline{\Phi},N,H}\left(\underline{a}|\underline{\phi}, n, h_1\right) = \prod_{i=1}^{n} f_{A|\underline{\Phi},H}\left(a_i|\underline{\phi}, h_i\right). \tag{4}$$

The vector $\underline{\Phi}$ captures the signal source components that are shared through observations at all active sensor nodes. One consequence is that such a network could infer only the radial component of the signal source's location from sensor observations. In a practical setting, the sensor deployments and signal propagation loss functions may not be rotation-independent. In which case, orientation may also be inferred from observations given an appropriate model. While $\underline{\Phi}$ (and realization $\underline{\phi}$) represents a vector of the signal source parameters, specifically the signal level and range to the origin of $\mathcal{R}$, we loosely refer to $\underline{\Phi}$ (and $\underline{\phi}$) as the signal.

For the given model, it follows that the sensor observations are conditionally i.i.d. according to

$$f_{\underline{X}|\underline{\Phi},N,H}\left(\underline{x}|\underline{\phi}, n, h_1\right) = \prod_{i=1}^{n} f_{X|\underline{\Phi},H}\left(x_i|\underline{\phi}, h_1\right), \tag{5}$$

where $f_{X|\underline{\Phi},H}\left(x|\underline{\phi}, h_1\right) = \mathrm{E}\left(f_{X|A,\underline{\Phi},H}\left(x|A, \underline{\phi}, h_1\right)\right)$ and $\mathrm{E}(\cdot)$ denotes expectation (it is with respect to $A|\underline{\Phi}, H$ in this case). The probability distribution $f_{X|\underline{\Phi},H}\left(x_i|\underline{\phi}, h_1\right)$ corresponds to the conditional distribution of an observation at active node i under h_1 and given the signal $\underline{\phi}$. This sensor-level distribution is essentially the result of marginalizing the randomness in a sensor node's location – the randomness that remains in A_i after conditioning by $\underline{\Phi}$. Note that $\{X_i\}$ are conditionally independent of $\underline{\Phi}$ given h_0 is the true state. Thus, $f_{X|\underline{\Phi},H}\left(x|\underline{\phi}, h_0\right) = f_{X|H}\left(x|h_0\right)$.

It follows that under both hypotheses, the observations are conditionally i.i.d. across the sensor network for a given signal $\underline{\phi}$ and n sensor nodes.

Each active sensor node first makes a local binary decision and then communicates that decision to a common fusion node. A local decision is a quantized or compressed version of the of the original observation. We consider two communications modes: a perfect communications model and a delay-constrained random access communications protocol.

2.2 Distributed Detections

Each active sensor node makes a local binary decision and communications that decision to a common fusion node. The local decisions are determined by an α_i-level decision rule, denoted by δ_i. The local decision rules δ_i are not necessarily identical across the sensor network in optimal fusion of binary decisions, even when observations are conditionally i.i.d. [7]. However, we assume each sensor shares a common α-level rule δ. This choice dramatically simplifies the design and deployment of the sensor network, and in some cases, proves to be asymptotically optimal for binary decisions [8].

The parameter $\alpha \in (0, 1)$ represents the local probability of false alarm. The local probability of missed detection, denoted by β, is given by

$$\beta = 1 - \mathrm{E}\left(\delta(X)|h_1\right). \tag{6}$$

We denote the local decisions by $Y_i \in \{h_0, h_1\}$ for $i = 1, 2, \ldots, N$. We refer to $Y_i = h_1$ as a local detection, whether it is a true ($H = h_1$) detection or a false ($H = h_0$) detection. Each Y_i conditioned on $\underline{\Phi}, N, H$ can be seen as a Bernoulli random variable with success probability $p_j\left(\delta|\underline{\phi}\right)$ defined by

$$p_j\left(\delta|\underline{\phi}\right) = \mathrm{E}\left(\delta(X)|\underline{\phi}, h_j\right), \tag{7}$$

for $j \in \{0, 1\}$. The success probabilities can be viewed as the conditional probabilities of false alarm ($j = 0$) and detection ($j = 1$) for decision rule δ and signal $\underline{\phi}$. When convenient, we suppress the dependence on δ by the local probabilities of detection and false alarm and simply write $p_1\left(\underline{\phi}\right) = p_1\left(\delta|\underline{\phi}\right)$ and $p_0\left(\underline{\phi}\right) = p_0\left(\delta|\underline{\phi}\right)$, respectively. Note that value $p_0\left(\underline{\phi}\right) = \alpha$ and does not depend on $\underline{\phi}$, while the decision region for δ may.

The conditional joint distribution of the binary decisions $\underline{Y}|\underline{\Phi}, N, H$ is then given by

$$f_{\underline{Y}|\underline{\Phi},N,H}\left(\underline{y}|\underline{\phi}, n, h_j\right) = \begin{cases} p_j\left(\underline{\phi}\right)^z \left[1 - p_j\left(\underline{\phi}\right)\right]^{n-z}, & z \leq n \\ 0, & z > n, \end{cases} \tag{8}$$

for $n \in \mathbb{N}_0$, $j \in \{0, 1\}$, and where $z = \sum_{i=1}^{n} 1(y_i = h_1)$ and $1(\cdot)$ is the indicator function. The joint probability distribution of $\underline{Y}, N|\underline{\phi}, H$ is then

$$f_{\underline{Y},N|\underline{\Phi},H}(\underline{y}, n|\underline{\phi}, h_j) = p_j\left(\underline{\phi}\right)^z \left[1 - p_j\left(\underline{\phi}\right)\right]^{n-z} e^{-\lambda}\frac{\lambda^n}{n!}, \tag{9}$$

for $z \leq n$. Let $Z = \sum_{i=1}^{N} 1(Y_i = h_1)$. For n active nodes and $z \leq n$ detections, there are $\binom{n}{z}$ different $\underline{y}$ that satisfy $\sum_{i=1}^{n} 1(y_i = h_1) = z$ with equal probability. It follows that the probability distribution of $Z, N|H$ is given by

$$f_{Z,N|\underline{\Phi},H}(z, n|\underline{\phi}, h_j) = \binom{n}{z} p_j\left(\underline{\phi}\right)^z \left[1 - p_j\left(\underline{\phi}\right)\right]^{n-z} e^{-\lambda}\frac{\lambda}{n!}^n, \tag{10}$$

for $z \leq n < \infty$. Marginalizing N, the number of active nodes, the conditional distribution of $Z|\underline{\Phi}, H$ is then given by

$$f_{Z|\underline{\Phi},H}(z|\underline{\phi}, h_j) = e^{-\lambda p_j(\underline{\phi})}\frac{\left[\lambda p_j\left(\underline{\phi}\right)\right]^z}{z!}, \tag{11}$$

for $z \in \mathbb{N}_0$. Note that the dependence on $\underline{\Phi}$ in equations 7 through 11 drops out under hypothesis h_0.

Recall that the active sensor network represents a homogeneous PPP and the number of active nodes is Poisson with mean λ. It follows by the thinning property of a PPP that $Z|\underline{\Phi}, H$ is a Poisson random variable with parameter $\lambda p_j\left(\underline{\phi}\right)$ under h_j and given $\underline{\Phi} = \underline{\phi}$.

2.3 Network Communication: Protocol Model

In this section, we describe a delay-constrained MAC protocol model. The local decisions Y_i, for $i = 1, 2, \ldots, N$, are communicated to a fusion node. The fusion node then combines received information to make a global decision as to the presence or absence of a signal source. The global decision rule must account for the effects in communications.

Sensor nodes are either awake or asleep during an activity period, which is formed by a sensing period followed by a communicating period. The sensing and communicating periods are synchronized so that each active sensor node observes the environment and makes a local

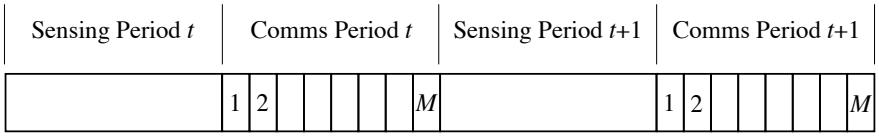

Figure 2. Activity periods composed of a sensing period and a communicating period for all active sensor nodes.

decision during the sensing period. Then, nodes attempt to transmit their decisions to a common fusion node during the communicating period. Figure 2 graphically depicts the sensing and communicating periods. Note that there could be overlap between a communicating period and the next sensing period, assuming one does not interfere with the other and so that similar periods do not overlap (e.g., Sensing Period t does not overlap with Sensing Period $t + 1$). We model the system as being time-invariant. Thus, we need only model a single activity period.

To both save transmission energy and reduce communication collisions, sensor nodes only transmit detections (i.e., when $Y_i = h_1$). Furthermore, the detection messages do not need to be unique to the sensor nodes. In references 4 and 5, similar distributed detection models were considered, but a transmitted decision can represent either h_0 or h_1. Here, messages to be transmitted represent only $Y_i = h_1$ decisions. In addition, we assume sensor nodes do not retransmit messages in the event of a collision, again to conserve energy. Since transmitted messages only represent detections, collisions provide valuable information at the fusion node.

During the communicating period, each sensor with a detection attempts to transmit a single detection message via Slotted ALOHA (S-ALOHA). The communicating period is broken into $1 \leq M < \infty$ equal-duration slots. On the receiving side, the fusion node does not know which slots will be used, so it must wait the duration of all M slots during the communicating period before making a decision. Thus, the communications delay is directly proportional to M. The delay, and therefore the number of slots M, is specified according to the needs of the detection application. In a slight deviation from previous notation, M is not considered random.

Nodes with detections randomly choose one out of M slots, independent of all other nodes, according to the same probability distribution. Let S_i represent the slot number chosen by the i^{th} node. The slot numbers are then drawn according to $\Pr(S_i = m) = p_m$, for $m = 1, 2, \ldots, M$.

We assume the fusion node can detect collisions in any of the M slots. A message is considered to be received successfully in a slot if only one sensor node transmits in that slot. Otherwise, a slot is either unused or contains collisions. A slot with 2 or more transmissions is counted as 1

collision. We denote the number of sensor nodes that select slot m for transmitting a detection message by T_m, and U_m represents the observation in slot m at the fusion node. We also refer to T_m as the slot occupancy (i.e., the number of nodes attempting a transmission in the slot). The observations at the fusion node are then related to the slot occupancies according to:

$$U_m = \begin{cases} 0, & \text{if } T_m = 0 \\ 1, & \text{if } T_m = 1 \\ c, & \text{if } T_m > 1, \end{cases} \tag{12}$$

for $m = 1, 2, \ldots, M$ and where c signifies a collision in the slot. With regards to notation, the vector $\underline{U} = [U_1, U_2, \ldots, U_M]^{\mathrm{T}}$ represents the collection of observations at the fusion node at the end of the communicating period, and $\underline{u} = [u_1, u_2, \ldots, u_M]^{\mathrm{T}}$ is a particular realization of $\underline{U} \in \{0, 1, c\}^M$.

Given the number of nodes with transmissions, the slot occupancies do not depend on the signal $\underline{\Phi}$ or the hypothesis H. Since the slot numbers are selected i.i.d. across the nodes with detections, the probability of occupancy in slot m, conditioned on z transmissions, is given by

$$f_{T_m|Z}\left(k|z\right) = \begin{cases} \binom{z}{k} p_m^k (1-p_m)^{z-k}, & k \leq z \\ 0, & k > z, \end{cases} \tag{13}$$

for $k, z \in \mathbb{N}_0$. Under this network model, the system designer can select the distribution from which nodes choose slot numbers. For a discrete uniform distribution (i.e., $p_m = 1/M$ for $m = 1, 2, \ldots, M$), the slot occupancies become identically distributed across slots and the number of transmitting nodes are uniformly spread across slots. We assume the slots are chosen according to the uniform distribution for the remainder of this work.

The number of active nodes is unknown to the fusion node and the number of transmitting nodes are uniformly spread across slots. The slot occupancies represent a thinning of Poisson points represented by sensor nodes with detections by the proportion $\frac{1}{M}$. It is straightforward to show that the slot occupancies are conditionally i.i.d. and distributed according to

$$f_{T_m|\underline{\Phi},H}\left(k|\underline{\phi}, h_j\right) = e^{-\frac{\lambda}{M} p_j\left(\underline{\phi}\right)} \frac{\left[\frac{\lambda}{M} p_j\left(\underline{\phi}\right)\right]^k}{k!}, \tag{14}$$

for $k \in \mathbb{N}_0$. The fusion node observes $\underline{U} \in \{0, 1, c\}^M$ with slot occupancies mapped according to equation 12. The probability distribution of $\underline{U}|\underline{\Phi}, H$, after some simplification, is then given by

$$f_{\underline{U}|\underline{\Phi},H}\left(\underline{u}|\underline{\phi}, h_j\right) = \left(\pi_{0,j}\right)^{M-n_1-n_c} \left(\pi_{1,j}\right)^{n_1} \left(\pi_{c,j}\right)^{n_c}, \tag{15}$$

where $n_1 = \sum_{m=1}^{M} 1(u_m = 1)$ and $n_c = \sum_{m=1}^{M} 1(u_m = c)$ are just the counts of 1's and c's across slots, respectively, and

$$\begin{aligned}
\pi_{0,j} &= \Pr\left(T_m = 0 | \underline{\phi}, h_j\right) \\
\pi_{1,j} &= \Pr\left(T_m = 1 | \underline{\phi}, h_j\right) \\
\pi_{c,j} &= \Pr\left(T_m > 1 | \underline{\phi}, h_j\right).
\end{aligned} \tag{16}$$

The probability $\pi_{u,j}$ depends on the local decision rule δ under both hypotheses and the signal $\underline{\Phi}$ under h_1. These dependencies are not explicit in denoting the probabilities $\pi_{u,j}$ to simplify the notation, but are clear from equation 14.

We define the (random) counts $N_u = \sum_{m=1}^{M} 1(U_m = u)$. It is clear from equation 15 that the observation $\{N_1, N_c\}$ is equivalent to $\underline{U}$ for determining H. The observations at the fusion node are then just the counts of the 1's and c's.

---

3. Global Decision Rules

In this section, we derive the global decision rule (or fusion rule) for a given local decision rule. First, we derive the fusion rule assuming the local decisions are perfectly communicated to the fusion node. Then, we derive the fusion rule for the delay-constrained MAC protocol outlined in section 2.3.

The global decisions rules are determined by an $\bar{\alpha}$-level composite likelihood-ratio test. The form of the rule is the same throughout, given by

$$\bar{\delta}_{(i)}(B) = \begin{cases} 1, & \text{if } l_{(i)}(B) > \eta_{(i)} \\ \zeta_{(i)}, & \text{if } l_{(i)}(B) = \eta_{(i)} \\ 0, & \text{if } l_{(i)}(B) < \eta_{(i)}, \end{cases} \tag{17}$$

where (i) denotes the special case, B is drawn according to a probability distribution $f_{B|H}$, and $l_{(i)}$ is the likelihood ratio. The probabilities of false alarm and missed detection, respectively, are given by

$$\bar{\alpha}_{(i)} = \mathrm{E}\left(\bar{\delta}_{(i)}(B) | h_0\right) \tag{18}$$

and

$$\bar{\beta}_{(i)} = 1 - \mathrm{E}\left(\bar{\delta}_{(i)}(B)|h_1\right). \tag{19}$$

The threshold $\eta_{(i)} \geq 0$ and randomization parameter $\zeta_{(i)} \in [0,1]$ are chosen to satisfy

$$\min_{\bar{\delta}_{(i)}} \bar{\beta}_{(i)} \text{ s.t. } \bar{\alpha}_{(i)} = \bar{\alpha}, \tag{20}$$

for some $\bar{\alpha} \in (0,1)$. All fusion rules are subject to the same global false alarm probability $\bar{\alpha}$. The global rules are potentially suboptimal since the local decision rules are constrained to be identical across the network.

3.1 Perfect Channel

We first consider fusing the binary decisions from all active sensors assuming unconstrained and error-free communications. In other words, it is assumed the local decisions are received perfectly at the fusion node.

The fusion node observes $Z \in \mathbb{N}_0$, the number of active nodes with detections. From equation 11, the conditional likelihood ratio for the global decision rule $\bar{\delta}_{(1)}$ is given by

$$l_{(1)}(z|\underline{\phi}) = e^{-\lambda\left[p_1\left(\underline{\phi}\right)-\alpha\right]}\left[\frac{p_1\left(\underline{\phi}\right)}{\alpha}\right]^z, \tag{21}$$

for $\bar{\alpha}, \alpha \in (0,1)$. The threshold $\eta_{(1)}$ and the randomization parameter $\zeta_{(1)}$ are chosen to satisfy the $\bar{\alpha}$-level test with likelihood ratio $l_{(1)}(z) = \mathrm{E}(l_{(1)}(z|\underline{\Phi}))$.

3.2 Delay-Constrained MAC

Now we consider the fusion rule for the delay-constrained MAC protocol. The binary decisions are communicated to the fusion node with sensor nodes transmitting according to the MAC protocol over M slots. The fusion node forms the decision rule after receiving the observations upon completion of all M slots.

The fusion node observes $N_1, N_c \in \{0,1,\ldots,M\}$ with $N_1 + N_c \leq M$. The fusion node also observers the number of unused slots N_0, which is a known quantity given N_1, N_c, and M. From

equation 15, the conditional likelihood ratio for the global decision rule $\bar{\delta}_{(2)}$ is given by

$$l_{(2)}\left(n_1, n_c|\underline{\phi}\right) = \left[\frac{\pi_{0,1}}{\pi_{0,0}}\right]^{M-n_1-n_c} \left[\frac{\pi_{1,1}}{\pi_{1,0}}\right]^{n_1} \left[\frac{\pi_{c,1}}{\pi_{c,0}}\right]^{n_c}, \tag{22}$$

for $n_1 + n_c \leq M$, $\pi_{u,j} \neq 0$, $\bar{\alpha} \in (0,1)$ and $\alpha \in (0,1)$. The threshold $\eta_{(2)}$ and the randomization parameter $\zeta_{(2)}$ are chosen to satisfy the $\bar{\alpha}$-level test with likelihood ratio $l_{(2)}(n_1, n_c) = \mathrm{E}(l_{(2)}(n_1, n_c|\underline{\Phi}))$.

The likelihood ratios for both cases are summarized in table 1. The expectations are with respect to the random signal $\underline{\Phi}$. In each case, the decision rules are functions of count statistics: the number of active nodes with detections, the number of slots with a successful transmission, or the number of slots with collisions.

Table 1. Likelihood ratios of count statistics.

Perfect Communications	MAC Protocol
$l_{(1)}(z) = \mathrm{E}\left(e^{-\lambda[p_1(\underline{\Phi})-\alpha]}\left[\frac{p_1(\underline{\Phi})}{\alpha}\right]^z\right)$	$l_{(2)}(n_1, n_c) = \mathrm{E}\left(\left[\frac{\bar{\pi}_{0,1}}{\bar{\pi}_{0,0}}\right]^{M-n_1-n_c}\left[\frac{\bar{\pi}_{1,1}}{\bar{\pi}_{1,0}}\right]^{n_1}\left[\frac{\bar{\pi}_{c,1}}{\bar{\pi}_{c,0}}\right]^{n_c}\right)$

4. System Performance

In this section, we discuss the system performance as a function of the density of the sensor network and the number of communications slots. The coverage area remains fixed, thus the average number of active sensors is synonymous with density. The system performance is characterized in terms of average energy consumption and global probability of missed detections.

4.1 Energy Versus Sensor Network Density

The amount of energy consumed for wireless transmissions can be of the same order as that needed for sensing and processing [9]. For the analysis here, we simply assume these two levels are identical. A more thorough analytical study or one like reference 9 could be carried out for the specific system being deployed.

Let E represent the amount of energy consumed by a sensor node over a single sensing or communicating period. Let $\rho_0 = \Pr(H = h_0)$. It is straightforward to show that the average energy consumption across the sensor nodes, denoted $\bar{E}_s$, is

$$\bar{E}_s = \lambda[1 + \rho_0\alpha + (1 - \rho_0)(1 - \beta)]E, \tag{23}$$

where α and β are the local probabilities of false alarm and missed detection, respectively.

We assume that E is constant with sensor network density. In the single-hop setting here, the coverage area and the location of fusion node are fixed. It is assumed that E is the lowest amount needed so that any one node in the coverage area can reliably communicate with the fusion node. Collisions are permitted and no attempt is made to separate near and far transmitters. A constant E could have an impact on the fusion node's ability to differentiate between the three states in a slot: no transmission, one transmission, or a collision. We do not consider physical layer complexities here.

The fusion node must remain active for all communicating periods. The number of slots and communications rates remain fixed with respect to density. Thus, the amount of energy consumed by the fusion node remains constant with density. Let E_f denote the amount of energy consumed by the fusion node in any given activity period. The total average energy consumed by the sensor network in any particular activity period is then given by

$$E_t = \bar{E}_s + E_f. \tag{24}$$

We assume the signal source is mostly absent (i.e., $\pi_0 > 1/2$). Most activity periods do not contain a signal source, and so processing and message transmissions are usually due to false alarms. We constrain the sensor network by forcing $\lambda\alpha$, the average number of false alarms, to be constant as the density of the sensor network grows (i.e., $\alpha \to 0$ as $\lambda \to \infty$ s.t. $\lambda\alpha$ is constant). In a typical setting, β tends to 1 as α tends to 0. It follows then that the average per-node energy use declines as the sensor network density increases. So while the total average energy across the network grows with density, the per-sensor-node usage decreases and the fusion node's usage is fixed.

4.2 Error Probability Versus Sensor Network Density

Here, we analyze the global probability of missed detection while increasing sensor network density and fixing the average number of false alarms from the sensor nodes and fixing the global probability of false alarm. The probability of missed detection is discussed for both cases.

Condition 1. The local detection tests are such that the local conditional probability of detection $p_1\left(\delta|\underline{\phi}\right)$ is concave, non-decreasing in $\alpha \in (0,1)$ for all signals $\underline{\phi} \in \mathcal{P}$.

Condition 2. The sensor observations under h_0 and h_1 have the same support for all $\underline{\phi} \in \mathcal{P}$. This condition ensures that the limit $\lim_{\alpha\to 0} p_1\left(\underline{\phi}\right)$ exists. The following results can be easily extended, however tedious, with this condition removed.

4.2.1 Perfect Channel with Observation $\{Z\}$

Since $p_1\left(\underline{\phi}\right) \geq \alpha, \forall \underline{\phi} \in \mathcal{P}$, the conditional likelihood ratio $l_{(1)}(Z|\underline{\phi})$ is non-decreasing in Z. An equivalent test for this case is given by

$$\bar{\delta}_{(1)}(Z|\underline{\phi}) = \begin{cases} 1, & \text{if } Z > z_{(1)} \\ \zeta_{(1)}, & \text{if } Z = z_{(1)} \\ 0, & \text{if } Z < z_{(1)}, \end{cases} \tag{25}$$

where now $z_{(1)}$ and $\zeta_{(1)}$ are chosen to satisfy $\bar{\alpha}$. It is clear that the decision region for this $\bar{\alpha}$-level test does not depend on $\underline{\phi}$. Thus, the decision region for rule $\bar{\delta}_{(1)}(Z|\underline{\phi})$ that achieves $\bar{\alpha}$ under h_0 does so also for composite rule $\bar{\delta}_{(1)}(Z)$. Since the decision region for $\bar{\delta}_{(1)}(Z|\underline{\phi})$ does not depend on $\underline{\phi}$, we have $\beta_{(1)} = \mathrm{E}(\beta_{(1)}(\underline{\Phi}))$.

Let $\underline{\phi} \in \mathcal{P}$ be given. The conditional probability of missed detection is given by

$$\bar{\beta}_{(1)}(\underline{\phi}) = \sum_{z=0}^{z_{(1)}} e^{-\lambda p_1(\underline{\phi})} \frac{\left[\lambda p_1\left(\underline{\phi}\right)\right]^z}{z!} - \zeta_{(1)} e^{-\lambda p_1(\underline{\phi})} \frac{\left[\lambda p_1\left(\underline{\phi}\right)\right]^{z_{(1)}}}{z_{(1)}!}. \tag{26}$$

If $\bar{\alpha}$ is fixed and $\lambda\alpha$ is held constant as λ increases, then from equations 11 and 25 both $z_{(1)}$ and $\zeta_{(1)}$ are fixed. Then, any change in $\bar{\beta}_{(1)}(\underline{\phi})$ is due to a change in $\lambda p_1\left(\underline{\phi}\right)$.

Let $\mu = \lambda p_1\left(\underline{\phi}\right)$. It is straightforward to show that equation 26 is decreasing in μ. Thus, if μ is non-decreasing in λ for every $\underline{\phi} \in \mathcal{P}$, then $\bar{\beta}_{(1)}$ is non-increasing for λ. It remains to show that the average number of detections, $\lambda p_1\left(\underline{\phi}\right)$, is increasing in λ with the constraint that $\lambda\alpha$ remains fixed.

Let $0 < \lambda_1 < \lambda_2 < \infty$ and $0 < \alpha_2 < \alpha_1 < 1$ be such that $\lambda_1\alpha_1 = \lambda_2\alpha_2$. Additionally, let δ_1 and δ_2 be the local detection rules associated with α_1 and α_2, respectively. Since the local tests are concave for any given $\underline{\phi} \in \mathcal{P}$, we have

$$\frac{p_1(\delta_1|\underline{\phi})}{\alpha_1} \leq \frac{p_1(\delta_2|\underline{\phi})}{\alpha_2}, \tag{27}$$

with equality if and only if $p_1(\delta|\underline{\phi})$ is linear on $(0, \alpha_1)$. Subsequently, we have

$$\begin{aligned} \lambda_2 p_1(\delta_2|\underline{\phi}) - \lambda_1 p_1(\delta_1|\underline{\phi}) &\geq \left[\lambda_2\alpha_2 - \lambda_1\alpha_1\right] \frac{p_1(\delta_1|\underline{\phi})}{\alpha_1} \\ &= 0. \end{aligned} \tag{28}$$

In general, the average number of positive detections is non-decreasing in λ while $\lambda\alpha$ is constant. The average number of positive detections is constant only where the local ROC curves have a line segment meeting the origin. If, for example, the local ROC curve is differentiable, then the average number of positive detections is strictly increasing, and so the global probability of missed detection is strictly decreasing in λ for a fixed average number of false alarms.

4.2.2 MAC Protocol with Observation $\{N_1, N_c\}$

Now, we analyze the performance of the MAC protocol while increasing sensor network density.

Let $\mu = \lambda p_1(\underline{\phi})$ and M be finite and fixed. We show that $\bar{\beta}_{(2)}$ is decreasing in μ. The conditional likelihood ratio $l_{(2)}(i, j|\underline{\phi})$ is strictly increasing in each coordinate and thus $l_{(2)}(i, j)$ is strictly increasing in each coordinate. Also, the joint probability of $\{N_1, N_c|h_0\}$ remains fixed with respect to μ and does not depend on $\underline{\phi}$. Hence, the $\bar{\alpha}$-level decision region does not depend on μ

and $\underline{\phi}$. Hence, it suffices to show that $\bar{\beta}_{(2)}(\underline{\phi})$ is decreasing in μ.

Let $\mathcal{X} = \{(i,j) \in \{0,1,\ldots,M\}^2 | i+j \leq M\}$ denote the feasible set of points. Also, let $\mathcal{A} = \{(i,j) \in \mathcal{X} | l_{(2)}(i,j) \leq \eta_{(2)}\}$ denote the $\bar{\alpha}$-level acceptance region for h_0. Under the MAC protocol, the global probability of false alarm is given by

$$\bar{\alpha}_{(2)} = \sum_{\substack{i=0 \\ (i,j)\in\mathcal{X}}}^{M} \sum_{j=0}^{M} \bar{\delta}_{(2)}(i,j) \mathbf{Pr}(N_1 = i, N_c = j | h_0). \tag{29}$$

The threshold $\eta_{(2)}$ and randomization $\zeta_{(2)}$ satisfy the constraint $\bar{\alpha}_{(2)} = \bar{\alpha}$. The global probability of missed detection, conditioned on $\underline{\phi}$, is given by

$$\bar{\beta}_{(2)}(\underline{\phi}) = \sum_{\substack{i=0 \\ (i,j)\in\mathcal{X}}}^{M} \sum_{j=0}^{M} \left(1 - \bar{\delta}_{(2)}(i,j)\right) \mathbf{Pr}(N_1 = i, N_c = j | h_1, \underline{\phi}), \tag{30}$$

which is upper bounded by

$$\begin{aligned}
\bar{\beta}_{(2)}(\underline{\phi}) &\leq \sum_{\substack{i=0 \\ (i,j)\in\mathcal{A}}}^{M} \sum_{j=0}^{M} \mathbf{Pr}(N_1 = i, N_c = j | h_1, \underline{\phi}) && (31) \\
&= \sum_{\substack{i=0 \\ (i,j)\in\mathcal{A}}}^{M} \sum_{j=0}^{M} \frac{M!}{(M-i-j)!i!j!} (\pi_{0,1})^{M-i-j} (\pi_{1,1})^{i} (\pi_{c,1})^{j} && (32) \\
&= \sum_{\substack{i=0 \\ (i,j)\in\mathcal{A}}}^{M} \sum_{j=0}^{M} \frac{M!}{(M-i-j)!i!j!} e^{-\mu} \left(\frac{\mu}{M}\right)^{i} \left(\sum_{k=2}^{\infty} \frac{\left(\frac{\mu}{M}\right)^{k}}{k!}\right)^{j}. && (33)
\end{aligned}$$

Denote the upper bound by B. Differentiating B with respect to μ, we have

$$\frac{\mathrm{d}B}{\mathrm{d}\mu} = \sum_{\substack{i=0 \\ (i,j)\in\mathcal{A}}}^{M} \sum_{j=0}^{M} \mathbf{Pr}(N_1 = i, N_c = j | h_1, \underline{\phi}) \left(-1 + \frac{i}{\mu} + \frac{j}{M} \frac{e^{\mu/M} - 1}{e^{\mu/M} - 1 - \mu/M}\right). \tag{34}$$

The joint probability masses are strictly positive since $\pi_{u,1} > 0$, for $u \in \{0,1,c\}$. Assume $(0,M) \notin \mathcal{A}$ (Note: This point maximizes the likelihood ratio. For sufficiently small $\bar{\alpha}$, we can exclude this point from the acceptance region for h_0). Then, for a weak constraint on μ, we want

each term in the summation to be negative. Accordingly, we have the inequality

$$0 > -1 + \frac{i}{\mu} + \frac{j}{M}\frac{e^{\mu/M} - 1}{e^{\mu/M} - 1 - \mu/M}. \tag{35}$$

It can be shown that the second term on the right-hand side in the above inequality is less than the third term. Thus, any μ that satisfies the inequality with $i = 1$ and $j = M - 1$ also satisfies the inequality for any $(i, j) \in \mathcal{A}$. After rearranging terms and weakening the above inequality, we have the inequality

$$e^{\mu/M} - 2\mu + 1 > 0, \tag{36}$$

which is satisfied for sufficiently large μ since $\lim_{x\to\infty} e^{-x}x^K = 0$ for any fixed and finite K. In other words, the global probability of missed detection is strictly decreasing in μ provided the probability of a successful transmission in any slot satisfies $\pi_{1,1} = e^{-\mu/M}(\mu/M) < \frac{1}{2M}$. Note that $\pi_{1,1}$ is strictly decreasing in μ for $\mu > M$.

It remains to show that the point $(0, M)$ maximizes the likelihood ratio. It is sufficient to work with the conditional likelihood ratio for the same reasons discussed above. Since the conditional likelihood ratio is strictly increasing in its coordinates, one could compare each of the $M + 1$ points that satisfy $n_1 + n_c = M$ (i.e., the upper right boundary of feasible points). Instead, from the likelihood ratio in equation 22, we only need to show that the ratio $[\pi_{c,1}/\pi_{c,0}]/[\pi_{1,1}/\pi_{1,0}]$ is greater than unity. Assume $p_1(\underline{\phi}) > \alpha$ for at least one $\underline{\phi} \in \mathcal{P}$ with non-zero probability. Otherwise, $p_1(\underline{\phi}) = \alpha$ for all $\underline{\phi} \in \mathcal{P}$, with all the local tests being purely random guesses (i.e., no sensor data required).

Consider that $\underline{\phi}$. The ratio from the terms of the likelihood ratio can be written as

$$\frac{\pi_{c,1}\pi_{1,0}}{\pi_{c,0}\pi_{1,1}} = \frac{\sum_{k=2}^{\infty}\frac{(\lambda p_1/M)^k}{k!}e^{-\lambda\alpha/M}(\lambda\alpha/M)}{\sum_{k=2}^{\infty}\frac{(\lambda\alpha/M)^k}{k!}e^{-\lambda p_1/M}(\lambda p_1/M)} \tag{37}$$

$$= \frac{e^{\lambda p_1/M}\sum_{m=1}^{\infty}\frac{(\lambda p_1/M)^m}{(m+1)!}}{e^{\lambda\alpha/M}\sum_{m=1}^{\infty}\frac{(\lambda\alpha/M)^m}{(m+1)!}} \tag{38}$$

$$> 1, \tag{39}$$

where the inequality follows since $f(x) = e^x\sum_{k=1}^{\infty}\frac{x^k}{(k+1)!}$ is clearly increasing in $x \in \mathbb{R}^+$. Thus, the point $(0, M)$ is the unique feasible point that maximizes $l_{(2)}(n_1, n_c)$.

4.3 Error Probability Versus Number of Communications Slots

In this section, we analyze the performance of the fusion rule under the MAC protocol while increasing the number of communications slots M. Instead of using the analytic form of the probability of missed detection, we examine the asymptotic error rate for a given signal $\underline{\phi}$ and fixed and finite λ. For that, we appeal to the Chernoff-Stein Lemma [10].

For a given $\underline{\phi} \in \mathcal{P}$, each $U_1, U_2, \ldots, U_M$ are drawn i.i.d. from Q_0 or Q_1, where Q_j represents the trinomial distribution of $U_i \in \{0, 1, c\}$ under h_j for $j = 0, 1$ and $i = 0, 1, \ldots, M$. According to the Chernoff-Stein Lemma, the best exponent of probability of missed detection is given by

$$\lim_{M\to\infty} \frac{1}{M} \log \bar{\beta}(\underline{\phi}) = -D(Q_0||Q_1) \tag{40}$$

$$= -\sum_{u\in\{0,1,c\}} \pi_{u,0} \log \frac{\pi_{u,0}}{\pi_{u,1}}. \tag{41}$$

Let $x_0 = \lambda\alpha/M$ and $x_1 = \lambda p_1/M$. From the log-sum inequality, we have the following relations. The relative entropy of the trinomial is lower bounded by

$$D(Q_0||Q_1) \geq e^{-x_0} \log \frac{e^{-x_0}}{e^{-x_1}} + (1 - e^{-x_0}) \log \frac{(1 - e^{-x_0})}{(1 - e^{-x_1})} \tag{42}$$

$$= e^{-x_0} \left[x_1 - x_0 + \left(x_0 + \sum_{k=2}^{\infty} \frac{x_0^k}{k!} \right) \log \frac{e^{-x_0} \left(x_0 + \sum_{k=2}^{\infty} \frac{x_0^k}{k!} \right)}{e^{-x_1} \left(x_1 + \sum_{k=2}^{\infty} \frac{x_1^k}{k!} \right)} \right]. \tag{43}$$

The relative entropy of the trinomial is also upper bound according to

$$D(Q_0||Q_1) \leq \sum_{k=0}^{\infty} e^{-x_0} \frac{x_0^k}{k!} \log \frac{e^{-x_0} \frac{x_0^k}{k!}}{e^{-x_1} \frac{x_1^k}{k!}} \tag{44}$$

$$= x_1 - x_0 + x_0 \log \frac{x_0}{x_1} \tag{45}$$

$$= \frac{1}{M} D(P_0||P_1), \tag{46}$$

where P_0 and P_1 are Poisson distributions with mean $\lambda\alpha$ and λp_1 respectively. From equations 43 and 46, we have

$$\lim_{M\to\infty} M D(Q_0||Q_1) = D(P_0||P_1). \tag{47}$$

This limit is not unlike the performance of the perfect communications case. To make the link, we compare the asymptotic behavior of the MAC protocol to that of another system under perfect

communications with observations that converge in distribution to the Poisson case. Namely, the observations seen by the fusion center are binomial.

Let n be the number of sensor nodes, and the fusion node observes a sequence $Y_1, Y_2, \ldots, Y_n$. Each Y_i are conditionally i.i.d. and drawn from either B_0 under h_0 or B_1 under h_1. The distributions B_0 and B_1 correspond to binomial distributions with parameters $(n, p_a\alpha)$ under h_0 and $(n, p_a p_1)$, where $p_a \in (0, 1)$ is the probability of a sensor node being active. We let $p_a \to 0$ as $n \to \infty$ such that $np_a = \lambda$. It can be shown that the statistic $Z = \sum_i Y_i$ is a sufficient statistic for detection at the fusion node. It is well known that the conditional distributions of Z converge to Poisson distributions with means $\lambda\alpha$ and λp_1, respectively. Thus, the performance of this system converges to that of the perfect channel system discussed in previous sections. Additionally, the best exponent of the probability of missed detection as $n \to \infty$ is the negative of relative entropy given by

$$D(B_0||B_1) = p_a\alpha \log \frac{p_a\alpha}{p_a p_1} + (1 - p_a\alpha) \log \frac{1 - p_a\alpha}{1 - p_a p_1} \tag{48}$$

$$= p_a\alpha \log \frac{\alpha}{p_1} + (1 - p_a\alpha) \left(\sum_{k=1}^{\infty} \frac{(p_a p_1)^k}{k} - \sum_{k=1}^{\infty} \frac{(p_a\alpha)^k}{k} \right), \tag{49}$$

where the last equality follows from the Taylor series expansion of $\log(1 - x)$ for $|x| < 1$. From equation 49, we have

$$\lim_{n\to\infty} nD(B_0||B_1) = \lambda\alpha \log \frac{\alpha}{p_1} + \lambda p_1 - \lambda\alpha \tag{50}$$

$$= D(P_0||P_1). \tag{51}$$

5. Confidence Interval of ROC

In this section, we provide a confidence interval of the receiver operating characteristic (ROC). The confidence interval captures the variability of the ROC across realizations of the sensor network. The confidence interval of the ROC is derived using Hölder's inequality. It is a bound and not necessarily tight, but applies in very general cases where the uncertainty in the false alarm probability (i.e., horizontal variation in the ROC) is insignificant compared that of the detection probability.

Here, the sensor observations are independent of the target under the null hypothesis, thus there is

no variation in the global false alarm probability due to a random target. This is also true relative to the randomness of sensor node locations under the null hypothesis. The remaining variability in the global false alarm probability is due to the randomness in the number of active nodes. For the confidence interval, we assume there is no horizontal variation in the ROC due to the randomness in the number of active nodes. For a given number of active nodes, the count statistics at the fusion node are binomial (under perfect communications). Since the average number of false alarms from the sensor nodes is held constant (i.e., $\alpha \to 0$ as $\lambda \to \infty$ s.t. $\lambda\alpha$ is constant), these binomial distributions are well approximated by Poisson distributions as the density of the network increases. Thus, the confidence interval given here is a measure of only the vertical variance of the ROC.

For random variable $W \in \mathcal{W}$ and mapping $g : \mathcal{W} \to [a, b]$, with $-\infty < a < b < \infty$, the variance of $g(W)$ can be upper bounded by

$$\text{var}(g(W)) \leq \text{E}(g(W)) \left[\lim_{q \to \infty} \left(\int_{\mathcal{W}} (g(w))^q \text{d}F_W \right)^{1/q} - \text{E}(g(W)) \right]. \tag{52}$$

Let $P_{(i)}$ represent the (random) probability of detection for decision rule $\bar{\delta}_{(i)}$. The randomness in $P_{(i)}$ follows from variability in the number of active nodes, the locations of the sensor nodes and the signal source, and the signal intensity. Consider $P_{(i)}$ as a mapping of a random vector to the interval $[0, 1]$. The variance of the probability of detection is upper bounded by

$$\text{var}(P_{(i)}) \leq \bar{\beta}_{(i)} \left(1 - \bar{\beta}_{(i)}\right). \tag{53}$$

As the probability of missed detection tends toward the extremes, the confidence interval on the detection probability shrinks. Figure 3 plots an hypothetical ROC curve with corresponding confidence interval derived from equation 53. For the example in figure 3 and assuming a beta probability distribution for $P_{(i)}$ with mean $(1 - \bar{\beta}_{(i)})$ and variance $\bar{\beta}_{(i)}(1 - \bar{\beta}_{(i)})$, more than 99.8% of the outcomes have a detection probability greater than 0.5 with a false alarm probability of 2×10^{-5} (the average detection probability being approximately 0.88).

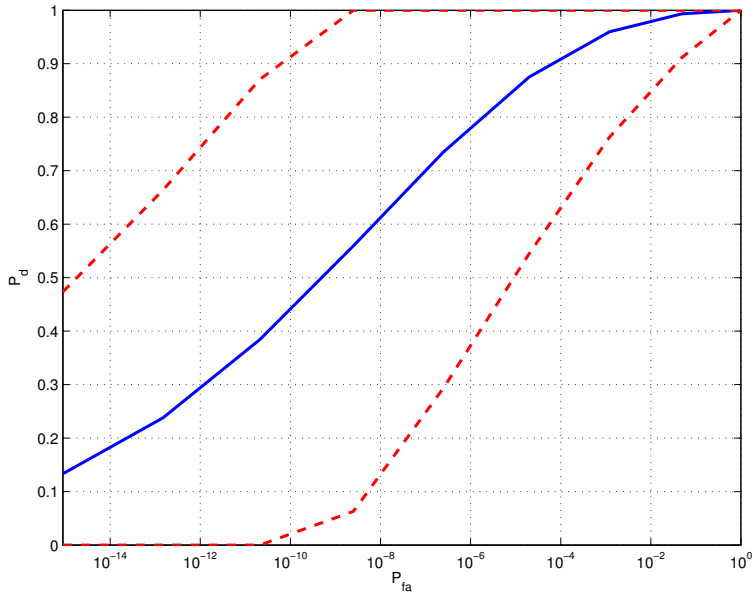

Figure 3. Notional ROC with 1σ confidence bounds.

6. Numerical Studies

In this section, we demonstrate system performance through numerical examples. The examples exhibit performance in terms of ROC curves, energy consumption, and probability of detection versus sensor network density and number of communicating slots.

The simulations parameters for the numerical example are as follows. The signal attenuation in the propagation medium is given by

$$g(d) = (d^2 + 1)^{-1} \tag{54}$$

where d is the distance between the sensor and signal source. This signal propagation loss model is very similar to those used in references 1, 2, 4, 5. The sensor observations under h_0 are chi-square distributed with 10 degrees of freedom. Under h_1, the sensor observations are (conditionally) noncentral chi-square distributed with 10 degrees of freedom and noncentrality parameter $10(A_s g\,(D))^2$, given the signal-sensor distance D and signal amplitude A_s. The sensor locations are uniformly distributed on a disk of radius $r = 20$ units. The range and amplitude of the signal source are modeled as discrete random variables. The distributions of the signal source's range R_s from the center of the disk and amplitude A_s are discrete uniforms on the intervals $[0, 20]$ and $[2, 200]$, respectively. The average number of false alarms is $\lambda\alpha = 10^{-1}$.

First, we compare the analytic ROC curves against sample estimates from 10^5 Monte Carlo trials for both cases: perfect communications and the delay-constrained MAC protocol. The ROC curves represent the global probability of detection versus global probability of false alarm. The purpose is to validate the analytic expressions since their evaluation involves numerical integration (due to the expectation with respect to random sensor locations). Figures 4-6 are plots of ROC curves, each with four different average number of active nodes: $\lambda = 10$ (blue), 20 (green), 40 (red), 80 (cyan) nodes. Figure 4 contains ROC curves for the perfect communications case. The solid lines represent the analytic curves and the circles are sample estimates of the ROC curves. Figure 5 contains ROC curves for the MAC protocol with $M = 3$ slots. The dashed lines in figure 5 represent the analytic curves and the circles are sample estimates of the ROC curves. As seen in figures 4 and 5, the sample estimates align well with the analytic forms. Each also demonstrate how the ROC curves improve with average number of nodes. The remaining simulation examples are evaluated from the analytic forms only.

Figure 6 overlays the analytic ROC curves of perfect communications (solid lines) and the MAC protocol (dashed lines) with $M = 3$ slots. The ROC curves in figure 6 are plotted on a smaller domain of probability of false alarm (i.e., $\bar{\alpha} \in (0, 10^{-3}]$) to show the slight reduction in performance from assuming perfect communications to the MAC protocol case, despite having only $M = 3$ slots for the protocol. Figure 9 demonstrates the detection probability versus a wider range of slots M. Recall that the fusion rules for each case are different and the fusion rule for the MAC protocol attempts retain as much information as possible from packet collisions. Fusion rules in the literature typically disregard slots with collisions.

Figure 7 represents the normalized per-node energy as a function of the average size of the sensor network. For this, we exclude the energy consumed by the fusion node since that amount remains constant. In particular, the normalized per-node energy is given by

$$\frac{\bar{E}_s}{\lambda E} = 1 + \rho_0 \alpha + (1 - \rho_0)\beta. \tag{55}$$

We do not assume a prior probability on the presence of a signal source. Thus, plotted in figure 7 are the extreme cases with $\rho_0 = 0$ (solid blue) and $\rho_0 = 1$ (dashed green). For either case, or any $\rho_0 \in (0, 1)$, this shows that the per-node energy expenditure decreases as the average number of sensor nodes increases. In particular, this is due to desensitizing the sensor nodes and therefore fewer nodes report detections to the fusion node.

Figure 8 demonstrates the improvement in the probability of detection as the average number of active nodes increases. Plotted are the probability of detection for perfect communications (solid

line) and the MAC protocol (dashed lines) for $M = 3$ ($\triangledown$), 5 ($\diamond$), and 7 ($\square$) slots, and with a probability of false alarm $\bar{\alpha} = 10^{-8}$. The probability of detection curve appears to flatten between 1000 and 3000 nodes. Although not shown, this is due to the choice of (discrete) distributions on the signal source. Roughly, about 90% of the signal sources have a probability of detection that increases from nearly 0 to 1 between 10 and 1000 nodes, while the other 10% do the same but for more than 3000 nodes. However, according to section 4.2.1, the increase in the detection probability is still strict since the local ROC curves are differentiable for this simulation example. It would not be a surprise that the support of and probability distribution of the signal source would have a significant impact on the performance of such a system.

Finally, figure 9 shows the probability of detection as a function of the number of communications slots M for the MAC protocol (squares) for $\lambda = 10$ (blue), 20 (green), 40 (red), 80 (cyan) nodes. The probability of false alarm is $\bar{\alpha} = 10^{-8}$. The solid lines represent the probability of detection assuming perfect communications, which does not depend on the number of slots. Figure 9 demonstrates that, even in the presence of collisions, performance approaches that of the ideal communications case for increasing number of slots. However, increasing the number of slots also increases the delay at the fusion node to make a global decision.

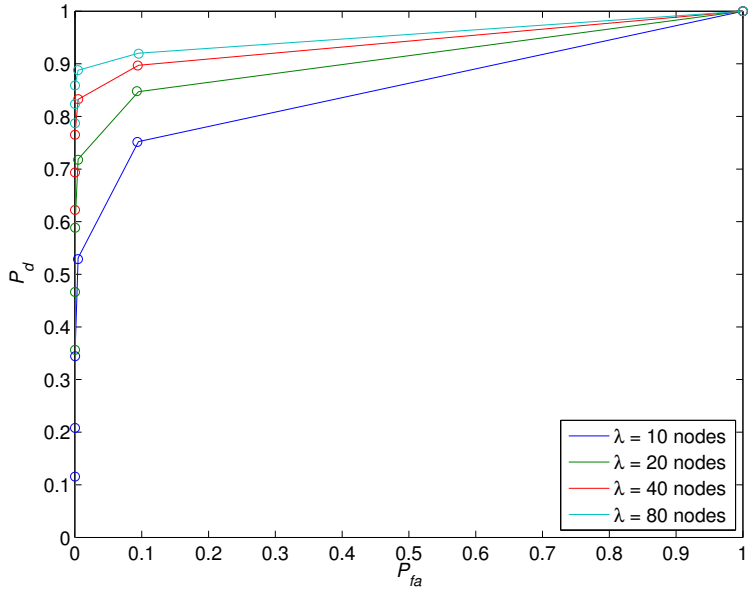

Figure 4. ROC curves for $\lambda = 10$ (blue), 20 (green), 40 (red), 80 (cyan) for perfect communications. Solid lines represent the analytic ROC and circles represent sample estimates.

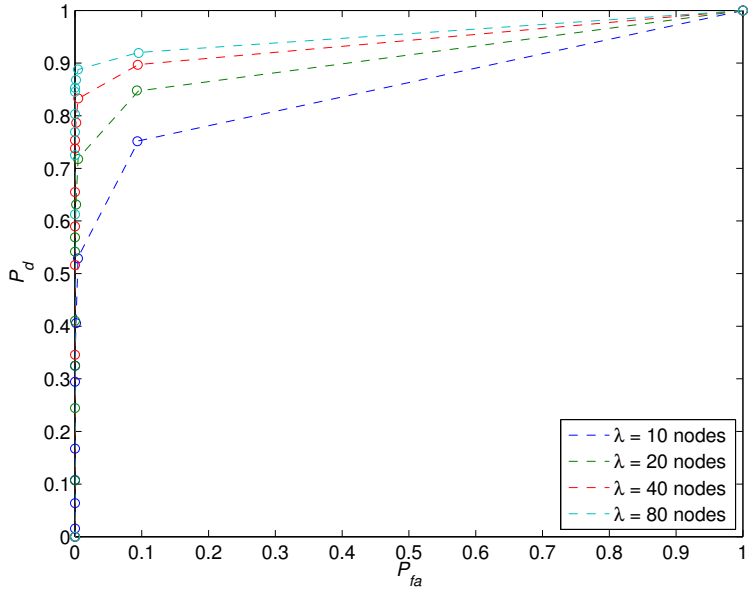

Figure 5. ROC curves for $\lambda = 10$ (blue), 20 (green), 40 (red), 80 (cyan) for the MAC protocol with $M = 3$ slots. Dashed lines represent the analytic ROC and circles represent sample estimates.

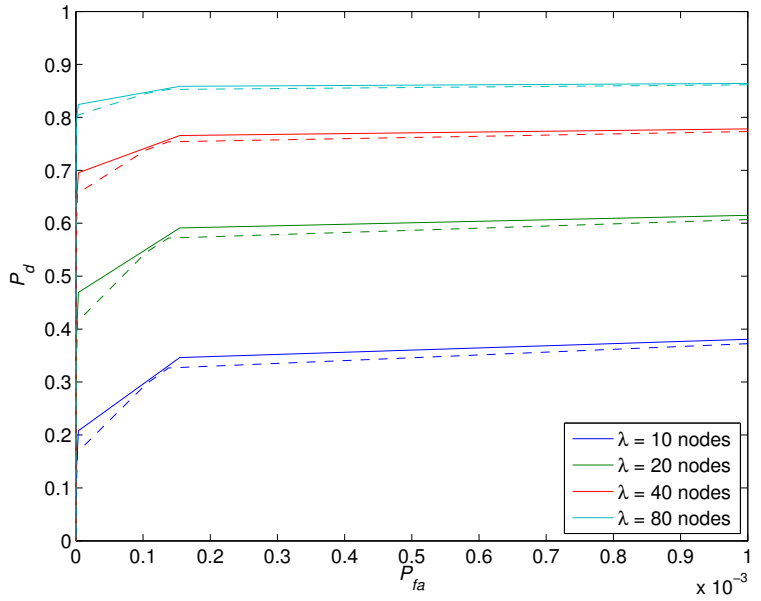

Figure 6. ROC curves for $\lambda = 10$ (blue), 20 (green), 40 (red), 80 (cyan). Solid and dashed lines represent the analytic ROC for perfect communications and the MAC protocol with $M = 3$ slots, respectively.

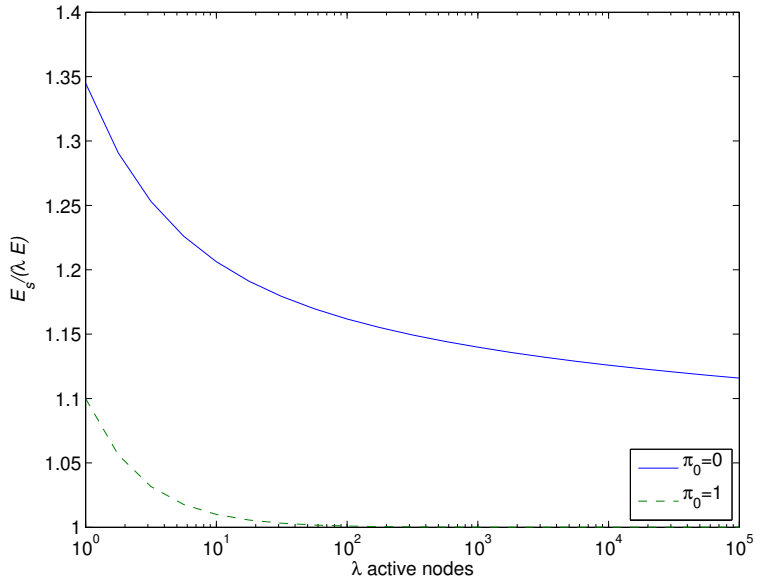

Figure 7. Normalized average per-node energy ($E_s/(\lambda E)$) versus number of active nodes λ assuming $\pi_0 = 0$ (solid blue) and $\pi_0 = 1$ (dashed green).

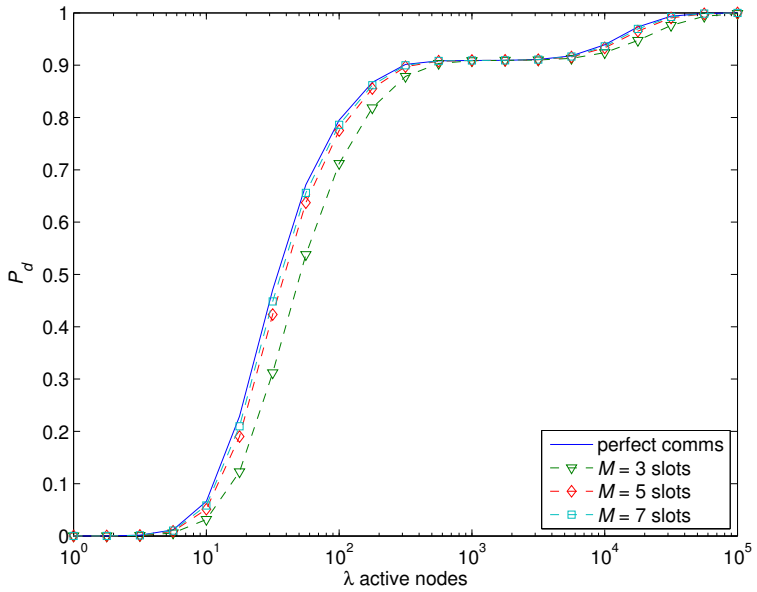

Figure 8. Global probability of detection versus number of active nodes λ for $P_{fa} = 10^{-8}$. The curves represent P_d for perfect communications (blue) and the MAC protocol with $M = 3$ (green), $M = 5$ (red), and $M = 7$ (cyan) slots.

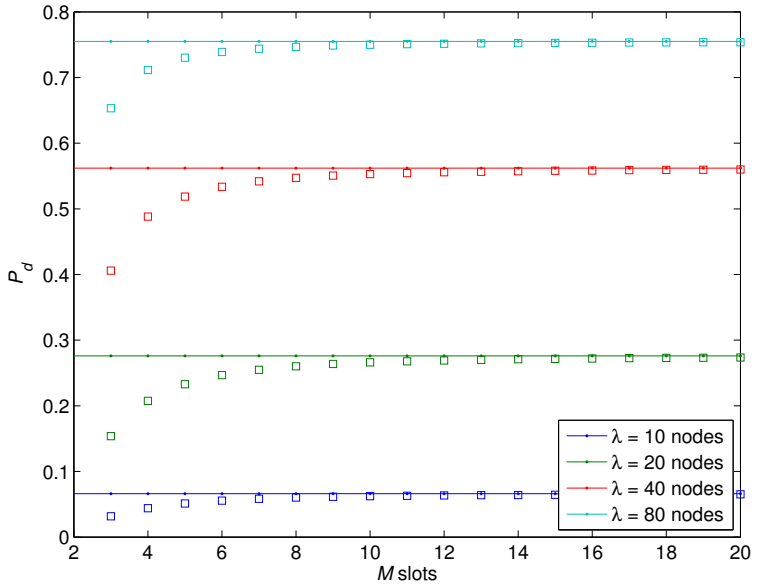

Figure 9. Global probability of detection versus number of communications slots M for $P_{fa} = 10^{-8}$ and $\lambda = 10$ (blue), 20 (green), 40 (red), 80 (cyan).

7. Conclusion

We derived the fusion rules for the case of sensor nodes communicating local binary decisions to a common fusion node for (1) assuming perfect communications and (2) through a delay-constrained random-access MAC on a single-hop wireless network. The fusion node combines received information to make a global decision on the presence or absence of a signal source. Under the MAC protocol, there is a chance that some detection messages are not received properly due to collisions with other messages since the communications medium is shared. In this work, sensor nodes attempt to transmit messages representing local detections only. Thus, collisions contain useful information about local detections. The fusion rules simply rely on count statistics: (1) the number of detections for perfect communications and (2) the number of successful transmissions and the number of collisions for the MAC protocol. The perfect communications case is seen as an asymptote of the MAC protocol case (i.e., as $M \to \infty$).

The local decision rules are constrained to be identical. Additionally, the system is constrained to maintain a constant number of false alarms across the sensor network in any given activity period. This implies that the sensor nodes are desensitized as the average number of active nodes increases. We showed that, for local decision rules that have concave ROC curves, the global detection performance improves with average number of active nodes, despite suppressing local decisions.

It was shown that the performance under the MAC protocol is somewhat degraded relative to the case of “ideal" communications. However, simulations show that the gap in performance can be negligible, despite collisions (without retransmissions) in communicating detection messages. Additionally, the gap in performance can be reduced by increasing the number of slots M, but at the expense of added delay.

In addition, we provided a bound on variance of the ROC curves. We assumed a random sensor network and signal source. The ROC curve for a given sensor network and signal source will vary from the average case. While the bound can be loose, it does not depend on the actual distributions and is simple to calculate for a given average-case ROC curve.

This framework could be extended to an asynchronous (or pure) ALOHA to reduce energy consumption in the sensor network. S-ALOHA requires time synchronization between all the sensor nodes and the fusion node. Additional procedures and communications are needed beyond those for signal detection to maintain synchronization within a desired tolerance. Removing the

need for synchronization also eliminates an energy budget associated with synchronization. However, it is well known that S-ALOHA reduces the probability of a collision over pure ALOHA due to halving of the vulnerability period. Thus, it is reasonable to conclude that the detection performance would be degraded compared to the MAC protocol discussed here.

8. References

1. Niu, R.; Varshney, P. K.; Cheng, Q. Distributed detection in a large wireless sensor network. *Special Issue on the Seventh Int. Conf. on Information Fusion-Part I* **2006**, *7* (4), 380 - 394.

2. Niu, R.; Varshney, P. Performance Analysis of Distributed Detection in a Random Sensor Field. *Signal Processing, IEEE Transactions on* **2008**, *56* (1), 339 -349.

3. Chang, T.-Y.; Hsu, T.-C.; Hong, P.-W. Exploiting Data-Dependent Transmission Control and MAC Timing Information for Distributed Detection in Sensor Networks. *Signal Processing, IEEE Transactions on* **2010**, *58* (3), 1369 -1382.

4. Kapnadak, V.; Coyle, E. Optimal density of sensors for distributed detection in single-hop wireless sensor networks. In *Information Fusion (FUSION), 2011 Proceedings of the 14th International Conference on*, Jul. 2011.

5. Aldalahmeh, S.; Ghogho, M.; Swami, A. Distributed detection of an unknown target in clustered wireless sensor networks. In *Signal Processing Advances in Wireless Communications (SPAWC), 2011 IEEE 12th International Workshop on*, Jun. 2011.

6. Fonseca, B.; Gubner, J. Analysis of randomly deployed sensor detection systems under least favorable distributions. In *Communication, Control, and Computing (Allerton), 2010 48th Annual Allerton Conference on*, 29 2010-oct. 1 2010.

7. Tenney, R. R.; Sandell, N. R. Detection with Distributed Sensors. *IEEE Trans. on Aerospace and Electronic Systems* **1981**, *17*, 501-510.

8. Tsitsiklis, J. N. Decentralized detection by a large number of sensors. *Mathematics of Control, Signals, and Systems (MCSS)* **1988**, *1*, 167-182; 10.1007/BF02551407.

9. Raghunathan, V.; Schurgers, C.; Park, S.; Srivastava, M. Energy-aware wireless microsensor networks. *Signal Processing Magazine, IEEE* **2002**, *19* (2), 40 -50.

10. Cover, T.; Thomas, J. *Elements of information theory*; 2 ed.; Wiley Series in Telecommunications and Signal Processing, Wiley-Interscience: 2006.

INTENTIONALLY LEFT BLANK.

NO. OF COPIES	ORGANIZATION
1 (PDF)	DEFENSE TECHNICAL INFORMATION CTR DTIC OCA
2 (PDF)	DIRECTOR US ARMY RESEARCH LAB RDRL CIO LL IMAL HRA MAIL & RECORDS MGMT
1 (PDF)	GOVT PRINTG OFC A MALHOTRA
5 (PDF)	DIRECTOR US ARMY RESEARCH LAB RDRL SES A JEMIN GEORGE LANCE M. KAPLAN TIEN PHAM NASSY SROUR GENE T. WHIPPS
2 (PDF)	THE OHIO STATE UNIVERSITY DEPARTMENT OF COMPUTER & ELECTRICAL ENGINEERING RANDOLPH L. MOSES EMRE ERTIN